Catalytically Active Monomer of Class Mu Glutathione Transferase from Rat†

Jennifer L. Hearne and Roberta F. Colman*

Department of Chemistry and Biochemistry, University of Delaware, Newark, Delaware 19716

Received February 6, 2006; Revised Manuscript Received March 21, 2006

ABSTRACT: Although rat glutathione transferase M1-1 is crystallized as a homodimer (GST M1-1), we have generated monomers (GST M1) of the enzyme by adding potassium bromide to buffer solutions containing the wild-type enzyme and by introducing point mutations in the electrostatic region of the subunit interface. The wild-type enzyme was evaluated in 0.05 M MES (pH 6.5) containing up to 3 M KBr. We report that the addition of KBr greatly influences the monomer−dimer equilibrium of the wild-type enzyme and that at 3 M KBr GST M1 has a specific activity close to that of GST M1-1. Since the effect of KBr is likely due to charge screening at the subunit interface, the influence on the monomer−dimer equilibrium exerted by the amino acid residues in the electrostatic region of the interface (Arg77, Asp97, Glu100, Asn101) was investigated. Mutations introduced at positions 97, 100, and 101 promote monomerization, resulting in enzymes that exhibit a decreased weight average molecular weight in comparison to that of the wild-type enzyme. However, only mutations at position 97 result in enzymes that have catalytic activity in the monomeric form. The mutations introduced at positions 100 or 101 result in enzymes whose activity can be accounted for by the amount of dimeric enzyme present. Our results indicate that the electrostatic region of the interface is important in the monomer−dimer equilibrium of glutathione transferase and that, although GST M1-1 may be more active than GST M1, the dimer is not *required* for catalytic function.

Cytosolic glutathione transferases (GSTs,[1] EC 2.5.1.18) constitute a ubiquitous family of enzymes involved in Phase II detoxification of xenobiotics (*1*) by catalyzing the nucleophilic addition of the thiolate of glutathione (GSH) to the electrophilic center of the xenobiotic compound. The conjugate is rendered more water soluble than the parent xenobiotic compound, which is advantageous for excretion, usually as part of the mercapturic pathway (*2*−*7*). Physiologically, glutathione transferases have been implicated in the protection against carcinogenesis as well as in drug resistance (*7*−*9*).

GST M1-1 belongs to the mu class of cytosolic GSTs, which has been crystallized as a homodimer with a molecular mass of ∼51 500 (*10*). Within each subunit of GST M1-1 there is an active site, consisting of the xenobiotic and glutathione sites, located along the V-shaped crevice formed between the subunits of the homodimer. Specifically, the CDNB site is composed of amino acid residues contributed by domain II of one subunit; in contrast, the glutathione site is composed of several amino acid residues contributed by domain I of the subunit to which GSH is bound and of one amino acid residue from domain II of the opposite subunit. In GST M1-1, Asp105 is the only amino acid residue contributed to the glutathione site from the opposite subunit to which GSH is bound (*11*). As depicted in Figure 1, the crystal structure shows two main areas of interaction between the two subunits: a hydrophobic region and an electrostatic region. The hydrophobic region, more commonly termed the "ball-and-socket", is located at each end of the subunit interface. This motif is well conserved in the alpha, mu, and pi classes of GSTs (*12*). In GST M1-1, this region consists of residues Val98, Tyr137, and Phe140 of one subunit forming the socket and Phe56 of its partner subunit forming the ball that intercalates among the socket residues. Hornby et al. (*13*) and Codreanu et al. (*14*) have extensively studied the importance of the hydrophobic region as an influence on the monomer−dimer equilibrium and have explored the relationship of the hydrophobic interactions to the enzyme's activity. The electrostatic region is situated along the dimer's 2-fold axis of symmetry (*C*2) between the two ball-and-socket regions (*13*).

Here, we focus on the electrostatic region of the interface. As shown in Figure 2, this region consists of amino acid residues Arg77, Asp97, and Glu100; in addition, we include Asn101, which has not previously been recognized as an amino acid residue located in the electrostatic region of the interface. These residues participate in intra- and intersubunit electrostatic interactions that can influence the monomer−dimer equilibrium of the enzyme. The closest intersubunit interaction, as measured *in silico*, is between the sym-

† This work was funded by NIH R01-CA66561 (R.F.C). The Beckman Optima XL-I analytical ultracentrifuge used in this study was obtained and supported by NIH 2P20 RR016472.

* To whom correspondence should be addressed. Phone: (302) 831-2973; fax: (302) 831-6335; e-mail: rfcolman@chem.udel.edu.

[1] Abbreviations: GST, glutathione transferase; WT, wild-type enzyme; GST M1-1, dimeric form of the wild-type enzyme; GST M1, monomeric form of the wild-type enzyme; GSH, glutathione; CDNB, 1-chloro-2,4-dinitrobenzene; TRIS, tris (hydroxymethyl) aminomethane; LB, Luria-Bertani; EDTA, disodium ethylenediamine tetraacetate; IPTG, isopropyl-β-D-thiogalactoside; CD, circular dichroism; MES, 2-(*N*-morpholino) ethane-sulphonic acid; KBr, potassium bromide; ESI-MS, electrospray ionization mass spectrometry; rpm, revolutions per minute.

10.1021/bi060249e CCC: $33.50
Published on Web 04/18/2006

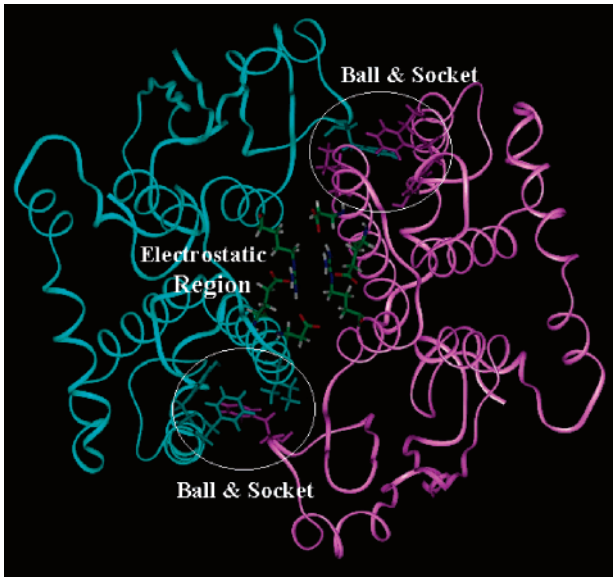

FIGURE 1: Dimeric structure of rat GST M1-1 (PDB 1GST) showing the two regions of interaction within the dimer interface. Subunit A is displayed in magenta and subunit B is in cyan. The ball-and-socket motif at each end of the dimer interface is accentuated by a white oval around its perimeter. The amino acid residues of the ball-and-socket motif are designated by color as to which subunit they are from. The amino acid residues of the electrostatic region, located in the center of the dimer interface, are colored by atom (oxygen in red, nitrogen in blue).

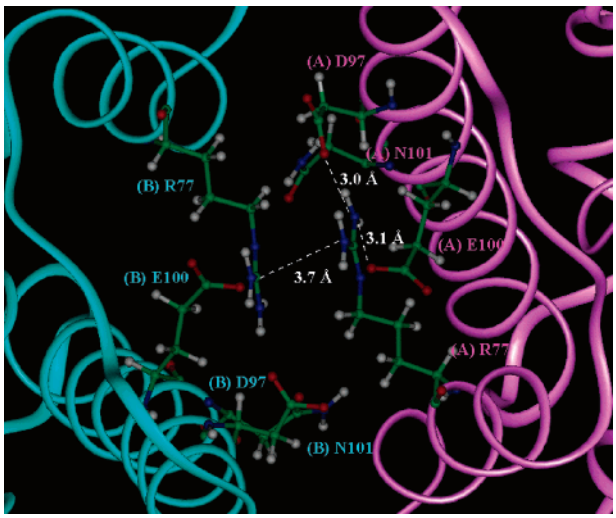

FIGURE 2: Enlargement of the electrostatic region of the dimer interface including N101 from both subunits. Subunit A is displayed in magenta, and subunit B is in cyan. The amino acid residues are colored by atom (oxygen in red, nitrogen in blue). The closest distances between some of the residues are shown.

metrically equivalent, stacked Arg77 amino acid residues of the two subunits (*15*−*17*), which are separated by only 3.7 Å (*10*). It is likely that the charge of Arg77 is neutralized within the subunit to which it belongs through electrostatic interactions with Asp97 and Glu100; this would allow hydrophobic interactions to take place between the arginine amino acid residues and prevent repulsion at the subunit interface. Within a subunit, Arg77 is only 3.0 Å from Asp97, 3.1 Å from Glu100, and 5.7 Å from Asn101 (Figure 2). In comparison, Arg77 of one subunit is 5.5 Å from Asp97, 5.6 Å from Glu100, and 8.2 Å from Asn101 of the opposite subunit. Using site-directed mutagenesis, we mutated each of these amino acid residues to evaluate their influence on the monomer−dimer equilibrium of the enzyme, as well as on the catalytic activity.

Furthermore, we sought to determine whether wild-type enzyme is active *only* in the dimeric form. Still focusing on the electrostatic interactions at the subunit interface, we subjected the wild-type enzyme to chaotropic salts, limiting the conditions to those in which the enzyme's activity could be measured. Our results indicate that monomers of the wild-type enzyme with catalytic activity can be generated under the defined chaotropic conditions, as well as by introducing single point mutations in the electrostatic region of the subunit interface.

EXPERIMENTAL PROCEDURES

Materials. Ampicillin, 1-chloro-2,4-dinitrobenzene (CDNB), GSH, MES, and *S*-hexylglutathione immobilized on cross-linked 4% agarose beads were purchased from Sigma Chemical Company. All other reagents were purchased from Fisher and were of reagent grade. The oligonucleotides for mutagenesis and the primers for DNA sequencing were purchased from Biosynthesis, Inc. The Quikchange XL Site-Directed Mutagenesis kit was obtained from Stratagene, and the QIAprep Spin Miniprep kit was supplied by QIAGEN.

Plasmid and Mutagenesis. The cDNA encoding *Rattus norvegicus* GST M1-1 (rat GST M1-1), as well as the 3′-untranslated region inserted into a pBR322 vector, was a generous gift from Ming F. Tam at the Institute of Molecular Biology, Academia Sinica, Nankang, Taipei, Taiwan. This plasmid was used with the permission of Dr. M. Rosenberg of Smith Kline Beecham, by whom the expression vector pMG27N (of which this is a derivative) was developed. Site-directed mutagenesis was accomplished using the Stratagene Quikchange XL Site-Directed Mutagenesis kit. The following oligonucleotides (written 5′- 3′) and their complementary sequences were used to incorporate the mutations into the cDNA. The mutated amino acid residue and number are marked in bold and the replacement codon is underlined: **R77E**, GC AAT GCC ATA ATG GAA TAC CTT GCC C; **R77Q**, GC AAT GCC ATA ATG CAG TAC CTT GCC C; **D97K**, CGG ATT CGT GCA AAA ATT GTG GAG AAC; **D97R**, CGG ATT CGT GCA CGC ATT GTG GAG AAC; **E100K**, GCA GAC ATT GTG AAA AAC CAG GTC ATG; **E100R**, GCA GAC ATT GTG CGC AAC CAG GTC ATG; **N101D**, GAC ATT GTG GAG GAT CAG GTC ATG; **N101K**, GAC ATT GTG GAG AAA CAG GTC ATG.

DNA extraction and purification was completed using the QIAprep Spin Miniprep kit. DNA sequencing was performed at the University of Delaware Center for Agricultural Biotechnology using an ABI Prism model 377 DNA sequencer (PE Biosystems) or an Applied Biosystems 3130 XL Genetic analyzer and confirmed the mutations. The forward sequencing primer is as follows: 5′ − ATG CCT ATG ATA CTG GGA TA − 3′ and the reverse primer is 5′ − CAT TGG GCC AAC TTC GAA AA − 3′. The mutant DNA was transformed into competent JM105 *Escherichia coli* (*E. coli*) cells for expression (*18*).

Protein Purification. The wild-type and mutant enzymes were expressed in JM105 *E. coli* cells. The cells were first grown at 37 °C in LB media containing 270 μM ampicillin until $A_{600\ nm}$ was 0.4−0.6 absorbance units, at which time

the enzymes were induced by the addition of 1 mM IPTG. The temperature was lowered to 25 °C, and the cells were allowed to grow for an additional 18 h and were then harvested by centrifugation at 10444*g* for 25 min at 4 °C. The resulting cell pellets were immediately frozen and stored at −80 °C. The cell pellet from 3 L of culture was thawed in a 25 °C water bath and resuspended in 30 mL of 10 mM TRIS chloride buffer (pH 7.8) at 25 °C. Six minutes of sonication (three 2-min intervals of sonication, separated by 30 s intervals) at 20 kHz and 475 W with a sonicator (Ultrasonic, Inc) was sufficient to rupture the cells. The suspension was kept on ice and then purified using chromatography on *S*-hexylglutathione agarose, as described previously by Hearne and Colman (*19*).

In addition, for the enzymes used in the presence of salt in 0.05 M MES (pH 6.5), the wild-type enzyme and the D97K mutant enzyme, were first purified as described above, after which the storage buffer [0.1 M potassium phosphate (pH 6.5) containing 1 mM EDTA] was exchanged for 0.05 M MES (pH 6.5) using the Amicon Ultra Centrifugal Filter Devices (Millipore Corp.). Twenty times the volume of the enzyme sample of 0.05 M MES (pH 6.5) was used to exchange the buffer. The enzyme concentration was determined using a HP 8453 UV−Vis spectrophotometer and the extinction coefficient at 270 nm ($\Delta\epsilon = 37\,700\ M^{-1}\ cm^{-1}$). The purity of the enzymes was assessed by N-terminal sequencing on an Applied Biosystems Procise Sequencing system (PE Biosystems).

Weight Average Molecular Weight Determination. A Beckman Coulter XL-I analytical ultracentrifuge was employed to determine the weight average molecular weight of each enzyme. Sedimentation equilibrium experiments at 10 °C were performed at speeds of 15 000, 17 000, and 20 000 rpm using an An-50 Ti rotor. Stepwise radial scans at 235 and 270 nm were performed after equilibrium was reached (*20*), using a step size of 0.001 cm. The resulting data sets were fitted using the software package IgorPro (Wavemetrics, Inc.), as previously described (*21*, *22*). The interface mutant enzyme samples (0.06−0.3 mg/mL) were in 0.1 M potassium phosphate buffer (pH 6.5) containing 1 mM EDTA and, when indicated, a saturating concentration of GSH was included. The addition of GSH to the enzyme samples was used to determine if this substrate would promote dimerization. The weight average molecular weight of each mutant enzyme in the presence of 2.5 or 5 mM GSH allowed us to calculate the percent dimer under conditions similar to the assay conditions used to determine V_{max}. We used 0.06 mg/mL enzyme samples since this is the lowest concentration yielding accurate weight average molecular weight data.

Sedimentation equilibrium experiments were also conducted under the same conditions for the wild-type enzyme samples (0.06−0.8 mg/mL) in 0.05 M MES (pH 6.5) containing various concentrations of KBr (0−3 M). The weight average molecular weight of each sample was also determined in the presence of a saturating GSH concentration. The densities of the buffers containing salt were considered in the calculations.

Circular Dichroism Spectroscopy. Circular dichroism spectroscopy was performed using a Jasco J-710 spectropolarimeter as previously described (*23*). The molar ellipticity of the enzyme sample [0.15 mg/mL in 0.1 M potassium phosphate buffer (pH 6.5) containing 1 mM EDTA] was measured as a function of wavelength between 200 and 250 nm at 0.2-nm increments. The average of five measurements was recorded as the spectrum. Each sample spectrum was corrected for the contribution from 0.1 M potassium phosphate buffer (pH 6.5) containing 1 mM EDTA. CD spectroscopy was not conducted when KBr was added to the MES buffer because of the high absorbance of the blank in the 200 nm to 250 nm range.

Enzymatic Assays. The K_m^{CDNB} was determined using a range of CDNB concentrations (5−1000 μM), while the GSH concentration was fixed at 2.5 mM (with a constant 2.5% ethanol). For those mutant enzymes that exhibited an elevated K_m^{CDNB} value, the CDNB concentration range was extended to 2.5 mM CDNB. Determination of the K_m^{GSH} for the CDNB−GSH conjugation reaction was conducted using a range of GSH concentrations (generally 10−2500 μM), while the 1 or 2.5 mM CDNB concentration was constant. For enzymes with unusually high K_m^{GSH} values, the range of GSH concentrations was extended to 20 mM. The enzymatic reactions (in 0.1 M potassium phosphate buffer (pH 6.5) containing 1 mM EDTA and 2.5% ethanol) were monitored at 340 nm ($\Delta\epsilon = 9.6\ mM^{-1}\ cm^{-1}$) using a Hewlett-Packard 8453 UV−Vis spectrophotometer (*24*). The specific activity of the enzymes is expressed as micromoles of substrate per minute per milligram of enzyme and is corrected for the rate of the spontaneous nonenzymatic conjugation reaction of CDNB and GSH. The reactions were maintained at 25 °C, and the conditions were generally saturating for the invariant substrate.

The kinetic parameters were determined for the wild-type enzyme in 0.05 M MES (pH 6.5) containing the various concentrations of KBr. For these measurements, the enzyme was stored in 0.05 M MES (pH 6.5) and was diluted into the assay buffer of 0.05 M MES (pH 6.5) and KBr immediately before the activity measurements. These kinetic studies were carried out as stated above except that all reactions were maintained at 10 °C to decrease the rate of the nonenzymatic reaction between CDNB and GSH. The data points were fitted to the Michaelis−Menten rectangular hyperbola using SigmaPlot. The standard errors of the V_{max} and K_m value determinations are reported in Results.

To test the stability of the wild-type enzyme in 0.05 M MES (pH 6.5) containing various concentrations of KBr, 0.3 mg/mL of the wild-type enzyme was incubated for 74 h in 0.05 M MES (pH 6.5) containing 0−3 M KBr at 10 °C. During this time, aliquots of the incubation mixtures were removed and assayed (2.5 mM GSH and 1 mM CDNB) in 0.05 M MES (pH 6.5) containing the same concentration of KBr as present in the incubation mixture. The assays were conducted at 10 °C.

Molecular Modeling. Molecular modeling was conducted using the Insight II (1997) software package from Molecular Simulations, Inc. on a Silicon Graphics Indigo 2 workstation. The atomic coordinates for the rat GST M1-1 isozyme were obtained from the Brookhaven Protein Databank, PDB 1GST (*10*). The mutant enzymes were modeled by replacing the individual amino acids at positions 77, 97, 100, and 101 with the amino acids corresponding to the mutations made at each position. In all cases, the enzyme structure was energy minimized by the Discover module of Biosym (Steepest

Table 1: CDNB and GSH Kinetic Parameters of the Wild-Type Enzyme in 0.05 M MES (pH6.5) Containing Various Concentrations of KBr

molarity KBr	V_{max}^{CDNB} (μmol min^{-1} mg^{-1})[a]	K_m^{CDNB} (μM)[a]	K_m^{GSH} (μM)[a]
0	22 ± 1	27 ± 2	86 ± 5
0.5	6.6 ± 0.2	120 ± 11	150 ± 11
1.0	6.6 ± 0.2	260 ± 15	240 ± 15
1.5	6.4 ± 0.2	340 ± 30	360 ± 38
2.0	6.4 ± 0.3	1000 ± 120	390 ± 33
2.5	5.3 ± 0.3	1100 ± 140	430 ± 37
3.0	5.5 ± 0.3	1800 ± 230	420 ± 26

[a] The K_m values were generally determined at 10 °C under saturating conditions of the invariant substrate, and the V_{max} values were determined by an extrapolation of the rate vs the concentration of the variable substrate kinetic data to infinite concentrations using SigmaPlot for data analysis. The data presented are the averages of two to four trials. The concentration of CDNB used in the determination of the K_m^{GSH} was 1 mM at 0−1.0 M KBr and 2.5 mM for the remaining KBr concentrations. The concentration of GSH used for the determination of K_m^{CDNB} was 2.5 mM for 0−1.5 M KBr and 5 mM GSH for the remaining KBr concentrations.

Gradient, 100 Iterations, 0.001 Derivative). The intermolecular energy was monitored for rational values and distances.

RESULTS

Expression and Purification. The plasmids encoding the wild-type or mutant glutathione transferase enzymes were expressed in JM105 *E. coli* cells, and the enzyme was purified using chromatography on *S*-hexylglutathione agarose. The purity of the enzymes was evaluated using N-terminal sequencing; in each case analysis indicated the presence of only one protein with the sequence PMILGYWNVRGL, which is unique to rat GST M1-1. The enzyme yield varied with the mutation; typically 15 mg/L cell culture was obtained of the wild-type enzyme and 2−23 mg/L cell culture of mutant enzyme.

Effect of KBr on the Wild-Type Enzyme. On the basis of the series of ions proposed by Hofmeister and Lewith in 1888, called the "Hofmeister series" (*25*), the wild-type enzyme was evaluated in 0.05 M MES (pH 6.5) in the absence and in the presence of potassium bromide (KBr). MES is a zwitterionic buffer and is not considered either a chaotropic or a kosmotropic ion, whereas the phosphate anion is considered a kosmotropic ion (*25*, *26*). Substitution of MES for the potassium phosphate buffer, used in our previous studies, allows us to evaluate the enzyme at the same pH. We chose to use the salt KBr because the bromide anion is an effective chaotropic ion, according to the Hofmeister series, and this salt allows us to keep the cation the same in the two buffer systems. We anticipated that this Hofmeister salt might shift the monomer−dimer equilibrium of the enzyme.

The wild-type enzyme was first characterized kinetically and biophysically in 0.05 M MES (pH 6.5) at 10 °C and compared to the wild-type enzyme in 0.1 M potassium phosphate (pH 6.5) containing 1 mM EDTA at 25 °C. As shown in Table 1, the kinetic parameters of the wild-type enzyme, which was stored in and assayed using 0.05 M MES (pH 6.5) (V_{max}^{CDNB} = 22 ± 1 μmol min^{-1} mg^{-1}, K_m^{CDNB} = 27 ± 2 μM, K_m^{GSH} = 86 ± 5 μM), are similar to those of wild-type stored and assayed in 0.1 M potassium phosphate (pH 6.5) containing 1 mM EDTA (Table 3). Sedimentation equilibrium experiments conducted at 0.3 mg/mL reveal that the enzyme's weight average molecular weight[2] in 0.05 M MES (pH 6.5) (Table 2, row 1) and 0.1 M potassium phosphate (pH 6.5) containing 1 mM EDTA (Table 4, row 1) are similar. Figure 3 is an example of the data obtained from the sedimentation equilibrium experiments. Thus, substitution of 0.05 M MES (pH 6.5) for 0.1 M potassium phosphate buffer (pH 6.5) containing 1 mM EDTA does not appreciably change the catalytic activity or the monomer−dimer equilibrium of the wild-type enzyme.

Table 2: Weight Average Molecular Weight of the Wild-Type Enzyme in 0.05 M MES (pH 6.5) Containing Various Concentrations of KBr, Determined in the Absence and in the Presence of Saturating GSH by Sedimentation Equilibrium Experiments

molarity, KBr[a]	weight average molecular weight (kDa)	weight average molecular weight with GSH (kDa)[b]
0	50.3 ± 0.1	47.8 ± 1.9
0.5	44.5 ± 0.4	45.5 ± 0.2
1.0	45.3 ± 0.1	46.2 ± 0.1
1.5	41.3 ± 0.3	41.4 ± 0.3
2.0	37.3 ± 0.3	39.6 ± 0.3
2.5	31.1 ± 0.4	31.6 ± 1.3
3.0	27.5 ± 0.9	26.1 ± 0.5

[a] In all cases, the enzyme (0.3 mg/mL) was in 0.05 M MES (pH 6.5) containing various concentrations of KBr and were run in the analytical ultracentrifuge at 10 °C. [b] The concentration of GSH (2.5−5 mM) was saturating.

Table 3: CDNB and GSH Kinetic Parameters of the Wild-Type and Mutant Enzymes[a]

enzyme	V_{max}^{CDNB} (μmol min^{-1} mg^{-1})	K_m^{CDNB} (μM)	K_m^{GSH} (μM)
WT	26 ± 3	19 ± 2	69 ± 9
D97K	1.1 ± 0.1	88 ± 5	230 ± 19
D97R	15 ± 1	52 ± 5	560 ± 56
E100K	14 ± 1	77 ± 10	2300 ± 170
E100R	18 ± 1	45 ± 7	780 ± 58
R77E	37 ± 1	28 ± 3	96 ± 7
R77Q	41 ± 1	20 ± 6	89 ± 3
N101D	230 ± 8	360 ± 56	390 ± 36
N101K	12 ± 1	360 ± 34	6600 ± 1600

[a] The K_m values were determined at 25 °C under saturating conditions of the invariant substrate, and the V_{max} values were determined by an extrapolation of the K_m kinetic data to infinite concentrations of CDNB using SigmaPlot for data analysis.

To promote monomerization, 0.5−3.0 M KBr was added to the wild-type enzyme in 0.05 M MES (pH 6.5). Table 2 shows that the average molecular weight of the wild-type enzyme in 0.05 M MES (pH 6.5) is dependent on the concentration of KBr present. The average molecular weights indicate that the enzyme is mostly dimeric at concentrations up to 1.0 M KBr (Table 2, rows 1−3). At 1.5 M KBr and above, the average molecular weight decreases as the concentration of KBr increases. The enzyme becomes predominantly monomeric (98.5%) in the presence of 3 M KBr (Table 2, row 7). The average molecular weight was evaluated in the absence and in the presence of saturating

[2] For ease of reading, we have substituted the term average molecular weight for weight average molecular weight.

Table 4: Weight Average Molecular Weights (expressed in kDa), as Determined by Sedimentation Equilibrium Experiments, of the Wild-Type Enzyme and Each Mutant Enzyme of the Electrostatic Region[a]

	0.06 mg/mL		0.3 mg/mL	
enzyme	−GSH	+GSH[b]	−GSH	+GSH[b]
WT	46.0 ± 0.3	46.9 ± 0.4	51.5 ± 0.1	51.7 ± 0.1
D97K	25.4 ± 0.1	26.3 ± 0.2	27.8 ± 0.1	27.6 ± 0.1
D97R	32.8 ± 0.2	36.0 ± 0.2	45.2 ± 0.3	44.0 ± 0.3
E100K	30.6 ± 0.2	39.6 ± 0.3	39.7 ± 0.3	44.4 ± 0.3
E100R	36.9 ± 0.1	47.3 ± 0.3	46.9 ± 0.1	49.7 ± 0.2
R77E	44.2 ± 1.3	50.8 ± 0.4	49.0 ± 0.1	49.5 ± 0.1
R77Q	47.5 ± 0.4	47.2 ± 0.2	48.6 ± 0.1	51.8 ± 0.9
N101D	46.0 ± 0.1	46.9 ± 0.2	51.5 ± 0.1	50.9 ± 0.1
N101K[b]	33.1 ± 0.1	35.3 ± 0.2	41.9 ± 0.1	43.8 ± 0.1

[a] The weight average molecular weights were determined in the absence and in the presence of GSH. In all cases, the enzyme was in 0.1 M potassium phosphate buffer (pH 6.5) containing 1 mM EDTA at 10 °C. [b] With the exception of the E100K and N101K mutant enzymes, the concentration of GSH (2.5 to 5 mM) was saturating.

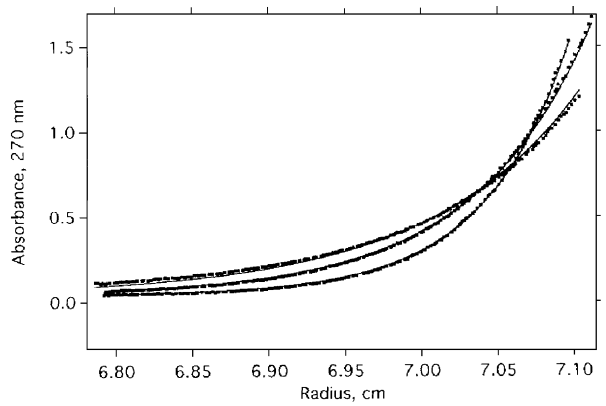

FIGURE 3: A representative sedimentation equilibrium data set collected using 0.24 mg/mL wild-type GST M1-1 and monitoring at 270 nm. The data sets shown are for three speeds: 15 000, 17 000, and 20 000 rpm; the curvature of the data is greater at the higher speeds.

GSH concentrations to determine if this substrate could promote dimerization. We find that GSH has little effect on the average molecular weight of the enzyme in the presence of KBr (Table 2).

Incubation of the wild-type enzyme over 74 h in 0.05 M MES (pH 6.5) containing 0−3 M KBr indicates that the enzyme, when assayed under the same salt conditions as those in the incubation solution, exhibits the same activity over the entire time period necessary to conduct the sedimentation equilibrium experiments (data not shown). Since there is no observable time dependence of change in enzymatic activity, we conclude that the activity of the wild-type enzyme in 0.05 M MES (pH 6.5) containing KBr is established rapidly and does not change over at least 74 h. Therefore, the average molecular weights of the wild-type enzyme samples under various concentrations of KBr are representative of the enzyme with the reported activities.

The kinetic parameters of the wild-type enzyme were evaluated at 0.5 M KBr increments. As shown in Table 1 (rows 1 and 2), the V_{max}^{CDNB} sharply decreases between 0 and 0.5 M KBr. The V_{max} values of the enzyme in the presence of 0.001 M through 0.4 M KBr were also determined (data not shown): the decrease in V_{max} is gradual between 0 and 0.1 M KBr, at which point the V_{max}^{CDNB} is equal to that of the enzyme in the presence of 0.5 M KBr. At concentrations greater than 0.5 M KBr the V_{max} values plateau at ~6.0 μmol min^{-1} mg^{-1} and do not deviate appreciably. In comparing the kinetic properties of the wild-type enzyme in the presence of 3 M KBr to the absence of KBr, there is a 4-fold decrease in V_{max}^{CDNB}, a 66-fold increase in the K_m^{CDNB}, and approximately a 5-fold increase in the enzyme's K_m^{GSH}. Examination of the k_{cat}/K_m^{GSH} and k_{cat}/K_m^{CDNB} reveals that the k_{cat}/K_m^{CDNB} is affected more than the k_{cat}/K_m^{GSH}. The k_{cat}/K_m^{CDNB} decreased approximately 270-fold, while the k_{cat}/K_m^{GSH} decreased approximately 20-fold. By comparing Tables 1 and 2, it becomes evident that the V_{max} of the GST M1-1 is not dependent on its average molecular weight. For example, at 0.5 M KBr, the wild-type enzyme exhibits a V_{max}^{CDNB} of 6.6 μmol min^{-1} mg^{-1} and an average molecular weight[2] of 45.3 ± 0.2 kDa in the presence of saturating glutathione. In comparison, at 3 M KBr, the wild-type enzyme exhibits a V_{max}^{CDNB} of 5.5 μmol min^{-1} mg^{-1} and an average molecular weight of 26.1 ± 0.5 kDa in the presence of a saturating concentration of glutathione.

Evaluation of Asp97. Since the addition of KBr to the buffer influenced the monomer−dimer equilibrium of the wild-type enzyme, most likely through a charge screening mechanism, the amino acid residues in the electrostatic region of the subunit interface were probed using site-directed mutagenesis. Asp97 was mutated to arginine (D97R) and lysine (D97K) to reverse the charge at this position. Table 3 (row 2) shows that the D97K mutant enzyme exhibits a 24-fold decrease in V_{max}^{CDNB}, accompanied by 5-fold increase in K_m^{CDNB} and 3-fold increase in K_m^{GSH} compared to those values of the wild-type enzyme (Table 3, row 1). The D97R mutant enzyme (Table 3, row 3) retains ~60% of the wild-type enzyme's V_{max}^{CDNB} value, but its K_m values increase approximately 3-fold for CDNB and 8-fold for GSH. The average molecular weight[2] (determined by sedimentation equilibrium studies) of each Asp97 mutant enzyme, in the absence and in the presence of glutathione (Table 4, rows 2 and 3), was considerably lower than that of the wild-type enzyme (Table 4, row 1). In the presence of 2.5 mM GSH, the D97K mutant enzyme (0.06 mg/mL) exhibits an average molecular weight of only 26.3 ± 0.2 kDa, a value equivalent to that of a monomer. At 0.06 mg/mL, the D97R mutant enzyme displays an average molecular weight of 36.0 ± 0.2 kDa, a value somewhat lower than that of the wild-type enzyme (46.9 ± 0.4 kDa) in the presence of saturating glutathione. To explore the possibility that the wild-type enzyme and the mutant enzymes' average molecular weight is dependent on the protein concentration, the average molecular weight of each mutant enzyme and the wild-type enzyme was also evaluated at 0.3 mg/mL (Table 4, rows 1−3). Indeed, the average molecular weights of these two mutant enzymes increase with increasing protein concentration (Figure 4A). The circular dichroism (CD) spectra of these mutant enzymes, shown in Figure 5A, reveal that the secondary structure of the D97K mutant enzyme exhibits a greater negative molar ellipticity than the wild-type enzyme, but the spectrum of the D97R mutant enzyme is similar to that of the wild-type enzyme. We attribute these changes in CD to the amino acid residue's propensity to be found in and form an alpha helix. Both aspartate and arginine have approximately the same helix propensity (*27*), while that of

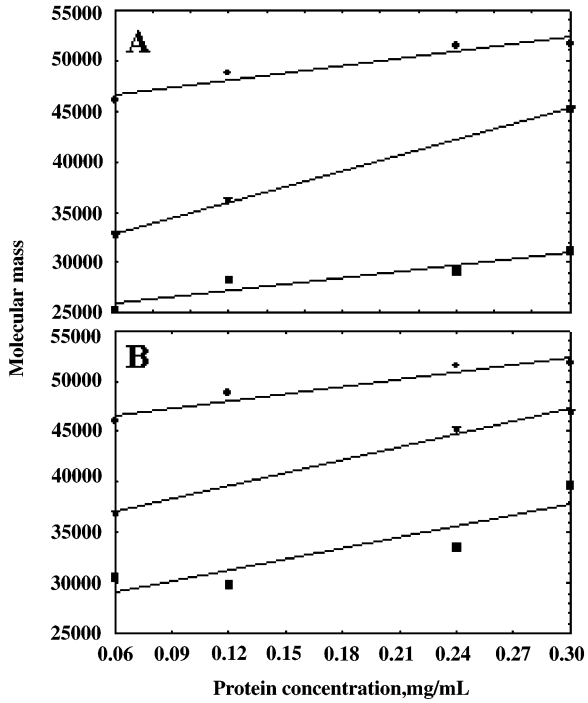

FIGURE 4: Graphical representation of the protein concentration dependence of wild-type GST M1-1 and the Asp97 and Glu100 mutant enzyme's weight average molecular weight in the absence of glutathione. (A) Wild-type enzyme (●), D97R (▼), D97K (■) and (B) wild-type enzyme (●), E100R (▼), and E100K (■).

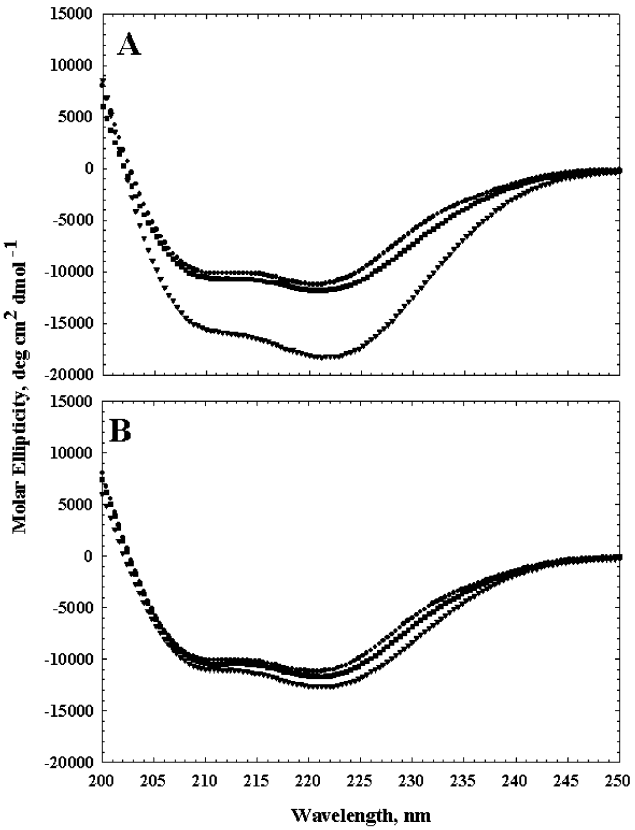

FIGURE 5: Circular dichroism spectra for wild-type enzyme and the mutant enzymes of positions 97 and 100. (A) Wild-type enzyme (●), D97K (▼), D97R (■). (B) Wild-type enzyme (●), E100K (▼), E100R (■).

lysine is greater. Collectively, these results indicate that changing the negative charge to a positive charge at position 97 significantly disrupts the electrostatic interactions at the subunit interface, causing changes in the secondary (D97K only) and quaternary structure of the enzymes, which in turn influences the enzymes' catalytic function.

Evaluation of Glu100. Glu100 was mutated to arginine (E100R) and lysine (E100K) to reverse the charge at this position. The kinetic parameters of each mutant enzyme are shown in Table 3 (rows 4 and 5). The largest change in kinetic parameters for the Glu100 mutant enzymes is in the K_m^{GSH}, which increases approximately 33-fold for the E100K mutant enzyme and 11-fold for the E100R mutant enzyme relative to the wild-type enzyme. Each mutant enzyme exhibits a decrease in V_{max}^{CDNB} as compared to the wild-type enzyme: to 69% for the E100R mutant enzyme and to 54% for the E100K mutant enzyme. The K_m^{CDNB} of the E100K mutant enzyme increases approximately 4-fold, and there is an approximate 2-fold increase in K_m^{CDNB} for the E100R mutant enzyme. To evaluate the quaternary structure of these mutant enzymes their weight average molecular weights[2] were determined by sedimentation equilibrium experiments. As shown in Table 4 (rows 4 and 5), the average molecular weight of the E100R mutant enzyme (47.3 ± 0.3 kDa) at 0.06 mg/mL in the presence of saturating glutathione is similar to that of the wild-type enzyme, while the E100K mutant enzyme (0.06 mg/mL) in the presence of saturating glutathione only reaches an average molecular weight of 39.6 ± 0.3 kDa. The average molecular weight of the Glu100 mutant enzymes is protein concentration dependent in the range tested (0.06 to 0.3 mg/mL) (Figure 4B). At 0.3 mg/mL, the average molecular weight of the E100K mutant enzyme is 39.7 ± 0.3 kDa, and the average molecular weight of the E100R mutant enzyme is 46.9 ± 0.1 kDa. As in the case of the Asp97 mutant enzymes, the E100K mutant enzyme displays a lower average molecular weight than the E100R mutant enzyme throughout the protein concentration range (Figure 4B). The secondary structures of these mutant enzymes are not appreciably different from that of the wild-type enzyme as determined by circular dichroism spectroscopy (Figure 5B). These results point out that, despite the lack of change in the secondary structures of the Glu100 mutant enzymes, the quaternary structure has been perturbed, and this perturbation of the quaternary structure is greater when glutamate is replaced with lysine than with arginine.

Evaluation of Arg77. Table 3 (rows 6 and 7) reveals that neither charge neutralization (R77Q) nor charge reversal (R77E) appreciably changes the kinetic parameters of these mutant enzymes in comparison to the wild-type enzyme. The results of the sedimentation equilibrium studies, shown in Table 4 (rows 6 and 7), in the absence or in the presence of 2.5 mM glutathione establishes that the R77E and the R77Q mutant enzymes have a weight average molecular weight similar to that of the wild-type enzyme and that the weight average molecular weights of these enzymes increase slightly as their concentrations are increased (0.06 to 0.3 mg/mL). Circular dichroism spectroscopy shows that the secondary structures of these two mutant enzymes are similar to that of the wild-type enzyme (Figure 6A). These results indicate that neither charge neutralization nor charge reversal perturbs the biophysical properties or kinetic parameters of the mutant enzymes relative to those of the wild-type enzyme. Therefore,

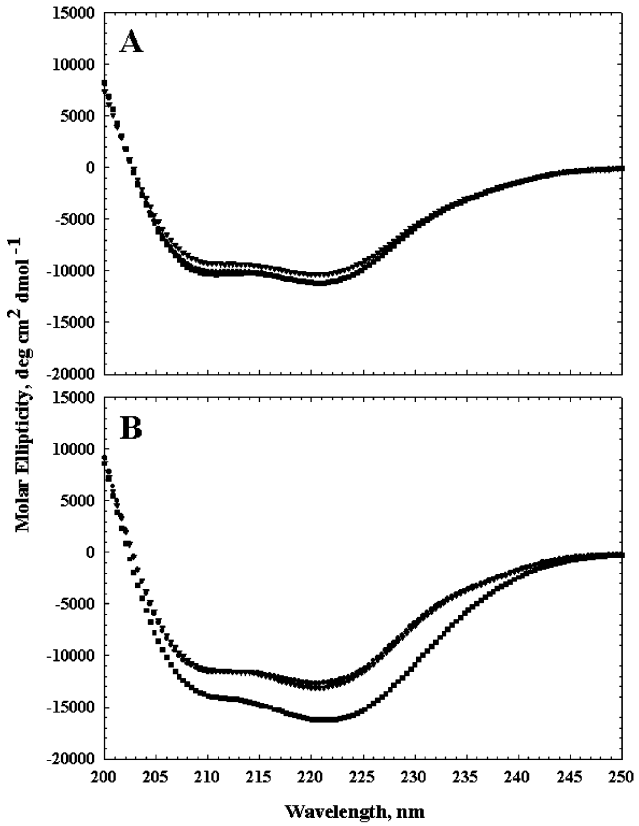

FIGURE 6: Circular dichroism spectra for wild-type enzyme and the mutant enzymes of positions 77 and 101. (A) Wild-type enzyme (●), R77E (▼), R77Q (■). (B) Wild-type enzyme (●), N101D (▼), N101K (■).

these amino acid changes do not disrupt the electrostatic interactions at the subunit interface.

Evaluation of Asn101. Although not previously recognized as an amino acid residue located in the electrostatic region of the subunit interface, Asn101 was mutated to the charged amino acid residues, aspartate and lysine. Introduction of a negative charge (N101D) increases all of the kinetic parameters studied compared to those of the wild-type enzyme (Table 3). The K_m values of the N101D mutant enzyme for GSH and CDNB increase about 6- and 19-fold, respectively, while the V_{max}^{CDNB} increases 9-fold (Table 3, rows 8 and 9). For the N101D mutant enzyme, the k_{cat}/K_m^{CDNB} decreases approximately 2-fold, while the k_{cat}/K_m^{GSH} increases approximately 2-fold. The replacement of the neutral asparagine by the positively charged lysine (N101K) has the opposite effect on V_{max}: it decreases the V_{max}^{CDNB} by 46% (Table 3, row 9). The largest change in kinetic parameters for the N101K mutant enzyme is the approximately 96-fold increase in K_m^{GSH}. The increase in K_m^{CDNB} for the N101K mutant enzyme is the same as it is for the N101D mutant enzyme. Table 4 (rows 8 and 9) displays the average molecular weight[2] of these two mutant enzymes at 0.06 and 0.3 mg/mL. The N101D mutant enzyme has an average molecular weight similar to that of the wild-type enzyme in the absence or in the presence of saturating glutathione, and its average molecular weight is dependent on the concentration of the protein within the range tested. In contrast, the N101K mutant enzyme at 0.06 and 0.3 mg/mL has an average molecular weight that is much lower than that of the wild-type enzyme, and its average molecular weight is dependent on the concentration of the enzyme (some data shown in Table 4). When the secondary structures of the mutant enzymes are examined by circular dichroism spectroscopy (Figure 6B), the N101D mutant enzyme's CD spectrum is similar to that of the wild-type enzyme, while the entire spectrum of the N101K mutant enzyme shows a greater magnitude of negative molar ellipticity than that of the wild-type enzyme (Figure 6B). As in the case of the D97 mutant enzymes, this change in the circular dichroism spectrum can be attributed to the likelihood of the residue to be in or form an alpha helix (*27*). The introduction of a charge at this position appreciably affects the kinetic parameters of the mutant enzymes when compared to those of the wild-type enzyme. However, only the replacement of Asn101 by lysine perturbs the secondary and quaternary structure of the enzyme.

DISCUSSION

Is there any evidence for a catalytically active monomer? This question has been explored as long as GSTs have been studied. Since both subunits of GST M1-1 contribute residues to the active site of the enzyme, it has been postulated that the dimeric form of the enzyme is required to maintain the functional conformation of the active site. Conversely, it has been shown that the monomeric intermediates of the wild-type enzyme have a nativelike secondary structure but display a less compact tertiary structure (*13*, *28*). Also, *in silico* homology modeling of GST M2-2 has revealed only small changes in conformation upon removal of a subunit (*29*). Therefore, it is reasonable to assume that under the appropriate conditions the monomeric form, GST M1, could be the predominant species and retain catalytic activity. Until now, conditions had not been determined under which catalytically competent monomers of the wild-type enzyme could be studied.

We established that 0.05 M MES (pH 6.5) containing a range of KBr concentrations was a satisfactory system for examining the monomer−dimer equilibrium of the wild-type enzyme. We found that as the concentration of KBr was increased the largest change in V_{max} was observed below 0.5 M KBr, while the change in the enzyme's average molecular weight[2] is observed at concentrations greater than or equal to 1.5 M KBr. Therefore, the decrease in the enzyme's activity is not due to the dissociation of the subunits but must be due to an effect of the salt on the enzyme's active site.

To calculate the activity of GST M1, we consider the parameters of the wild-type enzyme in the presence of 0.5 M KBr to be representative of the active, dimeric enzyme (GST M1-1). At 0.5 M KBr, the wild-type enzyme has a specific activity of 6.6 ± 0.2 μmol min^{-1} mg^{-1} and a weight average molecular weight of 45.5 ± 0.2 kDa in the presence of a saturating concentration of glutathione (at this average molecular weight[2] the enzyme is 76% dimeric). The percentage of the enzyme present in the dimeric form at the measured protein concentration (0.3 mg/mL) is calculated based on the definition of weight average molecular weight (M_w) [as stated by Freifelder (*30*) and Cantor and Schimmel (*31*)] and the measured weight average molecular weight (determined by sedimentation equilibrium experiments).

Assuming that all of the activity exhibited experimentally by the wild-type enzyme is due to the dimeric form of the enzyme, at 100% dimer the enzyme would be expected to

have a V_{max} of 8.7 μmol min^{-1} mg^{-1}. In comparison, at 3 M KBr, the wild-type enzyme exhibits experimentally a V_{max} of 5.5 μmol min^{-1} mg^{-1} and a weight average molecular weight of 26.1 $\pm$ 0.5 kDa in the presence of a saturating glutathione concentration. At this average molecular weight the enzyme is 1.5% dimeric. Again, assuming that only GST M1-1 is active and that the dimer has a V_{max} of 8.7 μmol min^{-1} mg^{-1}, in the presence of 3 M KBr, the enzyme would be expected to exhibit a V_{max} of approximately 0.1 μmol min^{-1} mg^{-1}; however, experimentally the enzyme exhibits a V_{max} of 5.5 μmol min^{-1} mg^{-1}. Therefore, it can be estimated that GST M1 has a V_{max} of 5.4 μmol min^{-1} mg^{-1}, which corresponds to 62% as much activity as GST M1-1, not accounting for the effects the salt exerts on the enzyme.

It has been established that the net charge of a protein can be reduced by ions (K^+, Br^-) acting to screen both favorable and repulsive interactions within the protein (*32*). This effect is commonly termed the screening effect, and it is important to the stability of a protein (*32*). The charge screening efficiency of a salt is generally in agreement with its ion's placement in the Hofmeister series (*33*). Therefore, the bromide anion should be efficient in reducing the net charge of the wild-type enzyme. We consider the effect of KBr on the monomer−dimer equilibrium of the wild-type enzyme to be through the Debye screening mechanism and not anion binding. Debye screening is comparatively nonspecific; KBr should reduce the strength of favorable and unfavorable interactions between the subunits, whereas anion binding should reduce the strength only of the unfavorable interactions among positively charged groups (*32*). The speculation that the effect of KBr is through Debye screening is supported by the fact that if only unfavorable interactions were screened we would expect the monomer−dimer equilibrium to either not change or shift more toward the dimeric state.

At the subunit interface of the wild-type enzyme, electrostatic and hydrophobic interactions are the major forces in stabilizing the dimeric protein (*13*, *14*, *26*, *28*). On the basis of our findings stated above, it is apparent that the electrostatic region of the wild-type enzyme greatly influences the monomer−dimer equilibrium of the enzyme. To determine the individual role of the amino acid residues in the electrostatic region of the subunit interface on the enzyme's monomer−dimer equilibrium, we constructed mutant enzymes using site-directed mutagenesis.

Replacement of Asp97 or Glu100 with either lysine or arginine places four positively charged amino acid residues (residues at positions 77 and 97 or 100 from both subunits) at the interface and thus most likely causes charge repulsion between the subunits resulting in mutant enzymes that display a decreased average molecular weight, with the exception of the E100R mutant enzyme. As modeled *in silico*,[3] the repulsion at the interface is partly caused by the repositioning of the Arg77 side chains, which is caused by a repulsive electrostatic interaction between the positively charged amino acid residue at position 97 or 100 and Arg77 within the same subunit. The repositioning of Arg77 perturbs the hydrophobic interactions of the two arginine amino acid residues across the interface and results in a repulsive electrostatic interaction between the guanidinium groups of the Arg77 side chains. It is evident by the average molecular weights exhibited by the Asp97 and Glu100 mutant enzymes that the point charge of lysine is more effective than the distributed charge of arginine in shifting the monomer−dimer equilibrium to favor the monomeric species. In the E100R mutant enzyme,[3] the unfavorable interaction between the Arg77 amino acid residues is most likely counteracted by a favorable electrostatic interaction between Arg100 of subunit A [(A)Arg100] and Asp97 of subunit B [(B)Asp97].

The shift in the monomer−dimer equilibrium of the N101K mutant enzyme[3] is probably due to charge repulsion at the subunit interface between the two lysine amino acid residues at position 101 (4.1 Å apart) in addition to the unfavorable electrostatic interaction of the Arg77 amino acid residues. The repositioning of Arg77 is due to charge repulsion within a subunit between (A)Lys101 and (A)Arg77.

Since Arg77 is the only positively charged amino acid residue that participates directly in the electrostatic region of the subunit interface, we expected that replacement of Arg77 with a negatively charged or neutral amino acid residue would change the electrostatic interactions at the subunit interface. However, substitution of this residue with a negatively charged or neutral amino acid residue results in enzymes with average molecular weights and kinetic parameters that are similar to those exhibited by the wild-type enzyme. These results differ greatly from those determined for the alpha class (*20*). Vargo et al. (*20*) found that Arg69 of GST A1-1, the equivalent of Arg77 of GST M1-1, was one of the most important residues affecting the monomer−dimer equilibrium of GST A1-1: the R69E mutant enzyme caused a marked decrease in the average molecular weight of GST A1-1. The close proximity between the amino acid residues contributing to the electrostatic region of the subunit interface and those comprising the GSH site in GST A1-1 provides the most probable explanation for the difference between the two classes of GSTs. In GST A1-1, (A)Arg69 neighbors (A)Thr68 and is close to (A)-Gln67, both of which hydrogen bond with (A)GSH (*20*). (A)-Thr68 hydrogen bonds with the α-carboxylate of (A)GSH and (A)Gln67 forms a hydrogen bond with the α-amino group of (A)GSH (*11*). (A)Arg69 interacts with (A)Glu104, which interacts with (A)Arg15 (*20*). In addition, Arg15 is unique to the alpha class of GSTs; its positive charge contributes to lowering the pK_a of the thiolate of GSH, thereby affecting the enzyme's catalytic properties (*20*). Although there are similar interactions in the mu class of GSTs, Arg77 of GST M1-1 is further from the GSH site than is Arg69 of GST A1-1.

To calculate the activity of the mutant GST M1 enzymes, we use the definition of weight average molecular weight summarized previously (*30*, *31*) and the following assumptions. In the presence of a saturating concentration of GSH and a protein concentration of 0.06 mg/mL, the wild-type enzyme is 82% dimeric and exhibits a V_{max} of 26 μmol min^{-1} mg^{-1}. Therefore, if the wild-type enzyme were 100% dimeric, the V_{max} would be expected to be 31.7 μmol min^{-1} mg^{-1}. For the D97R mutant enzyme under the same conditions [assuming that the dimeric form of the D97R

[3] The discussion of the mutant enzymes and their intra- and intersubunit distances is based on the determined crystal structure of the wild-type enzyme (PDB 1GST) in which a single amino acid in each case was mutated *in silico*, and the structure was subjected to energy minimization, as described in Experimental Procedures.

mutant enzyme (40%) accounts for all of the activity of the enzyme], 13 μmol min^{-1} mg^{-1} of the observed V_{max} of 15 μmol min^{-1} mg^{-1} is due to the dimer, leaving a mutant GST M1 monomer with a V_{max} of 2.0 μmol min^{-1} mg^{-1}. The weight average molecular weight of the D97K mutant enzyme at 0.06 mg/mL in the presence of 2.5 mM GSH is 26.3 $\pm$ 0.2 kDa, which is equivalent to 98% monomer. Under the same conditions as stated above, the monomeric form of the D97K mutant enzyme displays a specific activity of 0.5 μmol min^{-1} mg^{-1}. We conclude that both of the Asp97 mutant enzymes have some activity in their monomeric form; however, their activity is markedly decreased in comparison to the activity of the dimeric wild-type enzyme, GST M1-1. Mutating Glu100 and Asn101 to lysine shifts the monomer−dimer equilibrium to favor the monomeric state; however, all of the activity exhibited by these two mutant enzymes can be accounted for by the amount of dimeric enzyme present.

Since the D97K mutant enzyme has approximately the same percentage of the monomeric species as the wild-type enzyme does in the presence of 3 M KBr, we can compare the activities of the two. The activity of GST M1 is approximately 5.4 μmol min^{-1} mg^{-1} (in 3 M KBr) and that of the monomeric D97K mutant enzyme is approximately 0.5 μmol min^{-1} mg^{-1}. Therefore, the low activity of the monomeric D97K mutant enzyme is not due to the dissociation of the subunits but is caused by the substitution of lysine for aspartate. By comparing the wild-type enzyme and the D97K mutant enzyme in 0.05 M MES (pH 6.5), containing a range of KBr molarities (0−0.2 M), it is possible to account for the effects of the salt on the wild-type enzyme's activity. This comparison reveals that the decreased activity of the wild-type enzyme in 0.05 M MES (pH 6.5), in the presence of KBr is not due to the increased monomeric species but is due to an effect of the salt, since the D97K mutant enzyme lost approximately the same percentage of activity (~72%) as did the wild-type enzyme when subjected to increasing KBr concentrations (data not shown). The loss of activity is most likely due to the potassium and bromide ions electrostatically interacting with and thereby screening the amino acid residues that participate in the active site of the enzyme. Accounting for the decrease in V_{max} due to the salt, GST M1 is almost as active as GST M1-1.

Since these amino acid residues are clustered at the subunit interface away from the active site, the changes in the kinetic parameters of the Asp97, Glu100, and Asn101 mutant enzymes are probably the result of indirect effects perturbing the active site of the enzyme. With the exception of Asn101, the residues examined are at least 8 Å from the active site of the wild-type enzyme. Mutating these residues may indirectly disrupt the hydrogen bonding and electrostatic network in the vicinity of the active site, leading to local conformational changes.

Substitution of Asp97 by lysine or arginine reverses the charge and increases the size of the amino acid residue at this position. Although similar in size and charge, lysine and arginine have different effects on the enzyme's kinetic parameters and biophysical properties. Mills et al. (*34*) made similar observations upon substitution of lysine for arginine in Cytochrome *c* oxidase. In comparing the kinetic parameters of the D97R and D97K mutant enzymes, it is notable

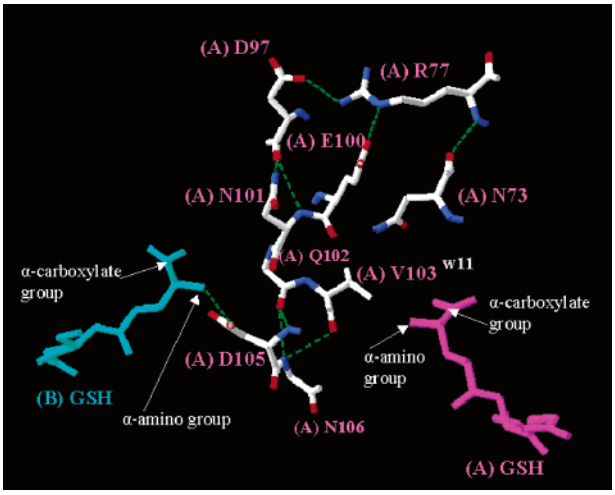

FIGURE 7: Hydrogen-bond network extending from the interface of the A subunit of GST M1-1 to the glutathione binding site in each subunit. GSH bound to the A subunit is colored in magenta, and GSH bound to the B subunit is colored in cyan. The amino acid residues are colored by atom, and the hydrogen bonds are shown in green. The glutathione molecules as well as the amino acid residues shown are denoted by (A) or (B) to correspond with the subunit they are contributed by. The side chains of 102 and 106 were not included (for clarity), and water molecule 11 is abbreviated as w11.

that the D97R mutant enzyme's K_m^{GSH} is approximately 2-fold greater than that of the D97K mutant enzyme; if the affinity of this enzyme for GSH were dependent on the dimeric form of the enzyme, then one would expect the opposite to be true since the D97K mutant enzyme is 98% monomeric and the D97R mutant enzyme is only 60% monomeric.

Figure 7 shows the interface region of the A subunit, with glutathione bound to both subunits. Since the D97K mutant enzyme is 98% monomeric, there can be no hydrogen bond between the side chain carboxylate of (A)Asp105 and the α-amino group of (B)GSH; thus, the monomeric structure of the D97K mutant enzyme may contribute to the increased K_m^{GSH} value. We postulate that the loss of this hydrogen bond may also be a factor in the markedly decreased V_{max} value exhibited by the D97K mutant enzyme. Adang et al. (*35*−*37*) reported that, when the α-amino group of GSH is lacking, the enzyme still uses the derivative as a substrate, but the V_{max} is decreased. In our case, the α-amino group of GSH is not lacking, but the hydrogen bond that ensures its proper orientation within the glutathione site is missing. The increased K_m^{GSH} exhibited by the D97K mutant enzyme, in comparison to the wild-type enzyme, may also be due to the disruption of an intrasubunit hydrogen-bond network extending from the interface to the glutathione site within the same subunit accompanied by a local conformational change. The introduction of lysine at position 97 would eliminate the hydrogen bond between the side chain carboxylate of (A)Asp97 and the guanidinium group of (A)-Arg77, and there would be electrostatic repulsion between (A)Lys97 and (A)Arg77 (Figure 7). This repulsion would perturb the hydrogen bond between the side chain carboxylate of (A)Glu100 and the side chain guanidinium of (A)-Arg77, as well as the hydrogen bond between the peptide backbone amide of (A)Arg77 and the peptide backbone carbonyl oxygen of (A)Asn73 (Figure 7 and ref *38*). In the

wild-type enzyme, the side chain amide of (A)Asn73 is 5.5 Å from the α-carboxylate group of (A)GSH; however, water 11 is within hydrogen-bonding distance of (A)GSH and (A)-Asn73, thus creating the potential for a water-mediated hydrogen-bond network. In the D97K mutant enzyme,[3] the distance from (A)Asn73 to (A)GSH is decreased to 2.9 Å, potentially allowing for a hydrogen bond to form directly between Asn73 and GSH. The distortion produced by the additional hydrogen bond from (A)Asn73 to (A)GSH may account for or contribute to the decrease in V_{max}.

The scenario for the D97R mutant enzyme[3] is similar except that the enzyme is only 60% monomeric. Therefore, the loss of the hydrogen bond from (B)Asp105 to the (A)-GSH site would contribute less to the increase in K_m^{GSH}, while the unfavorable interactions of the Arg77 and Arg97 residues would be relatively more important.

The increase in K_m^{GSH} for the E100K and E100R mutant enzymes[3] could be due to the proximity between the side chain ammonium of (A)Lys100 and the guanidinium group of (A)Arg77 (3.1 Å). The substitution of lysine or arginine at position 100 may disrupt the hydrogen-bonding network extending normally from the side chain carboxylate of (A)-Glu100 to GSH bound to the A subunit, as described for the Asp97 mutant enzymes. In addition, the E100K mutant enzyme is 46% monomeric; in the monomeric form, the hydrogen bond extending across the interface between (A)-Asp105 and (B)GSH is missing, thereby increasing the K_m^{GSH} of the E100K mutant enzyme more than that of the E100R mutant enzyme.

In the wild-type enzyme, the side chain oxygen of (A)-Asn101 is 5.6 Å from the α-carboxylate of (B)GSH. When aspartate replaces this asparagine, this distance is only slightly decreased to 5.1 Å[3]. However, the model of the N101D mutant enzyme[3] shows that there are two acidic amino acid residues, (A)Asp97 and (A)Glu100, as well as two neutral amino acid residues, (B)Asn73 and (A)Gln102, within 5 Å of the side chain carboxylate of (A)Asp101. The proximity between (A)Asp101 and these amino acid residues, as well as (B)GSH, allows for a cumulative repulsive electrostatic interaction that may increase the rate-limiting step of product release. This is the most probable explanation for the increased K_m^{GSH} and V_{max}. The increased K_m^{GSH} of the N101K mutant enzyme also could be due to a local conformational change in the GSH binding site of the N101K mutant enzyme. A lysine residue at position 101, (A)Lys101, may compete with (A)Arg77 in interacting with (A)Glu100[3]. As modeled *in silico* the lysine residue of the A subunit is only 4.5 Å from (A)Glu100, which is close enough for an electrostatic interaction to occur. If the electrostatic interaction were favored, the hydrogen-bond network extending from (A)Glu100 to (A)GSH (previously discussed) would be perturbed leading to an increased K_m^{GSH}.

While this paper was in the final stages of preparation, the report by Thompson et al. was published (*39*). These authors demonstrated that replacement of both Phe56, of the "ball-and-socket" hydrophobic region and Arg81 in the general region of the subunit interface yield a monomeric mutant rat GST M1 enzyme and that a single mutation at the subunit interface of GST M1-1 is sufficient to generate a monomeric mutant enzyme that exhibits a secondary structure similar to that of the wild-type enzyme; however, the catalytic activity of their monomeric mutant enzymes were markedly decreased. As shown above, we also determined that a single mutation in the electrostatic region of the subunit interface is sufficient to generate a monomeric species whose secondary structure is not appreciably perturbed. Of the interface mutant enzymes we examined in this report, only the D97K mutant enzyme exhibited activity in the monomeric form and the activity was markedly decreased. As discussed above, the decreased activity of the D97K mutant enzyme is attributed to intrasubunit changes rather than the generation of the monomeric species since we determined that, under the stated conditions, GST M1 was almost as active as GST M1-1.

GST M1-1 is crystallized as a dimer. In solution, we find that the enzyme is at equilibrium between the monomeric and dimeric species; the extent of either species is dependent on the solution conditions, the concentration of the enzyme, and whether a mutation has been made at the subunit interface. This paper demonstrates that GST M1 can be almost as active as GST M1-1 and that the electrostatic region of the subunit interface greatly influences the monomer−dimer equilibrium of the enzyme. Of the amino acid residues studied by site-directed mutagenesis, we find that Asp97 is the most influential for enzyme's monomer−dimer equilibrium.

ACKNOWLEDGMENT

We thank Dr. Ming Tam and Dr. M. Rosenberg for the plasmid and its use, Dr. Joel Schneider for the use of the IgorPro data analysis software, and Dr. Yu-Chu Huang for obtaining the N-terminal sequences.

REFERENCES

1. Jakoby, W. B., and Habig, W. H. (1980) *Enzymatic Basis of Detoxification* (Jakoby, W. B., Ed.) Vol. 2, pp 63−94, Academic, New York.
2. Mannervik, B., and Danielson, U. H. (1988) Glutathione transferases-structure and catalytic activity, *CRC Crit. Rev. Biochem. 23*, 283−337.
3. Boyer, T. D. (1989) The glutathione S-transferases: an update, *Hepatology 9*, 486-496.
4. Pickett, C. B., and Lu, A. Y. (1989) Glutathione S-transferases: gene structure, regulation, and biological function, *Annu. Rev. Biochem. 58*, 743−764.
5. Coles, B. and Ketterer, B. (1990) The role of glutathione and glutathione transferases in chemical carcinogenesis, *Crit. Rev. Biochem. Mol. Biol. 25*, 47−70.
6. Armstrong, R. N. (1991) Glutathione S-transferases: reaction mechanism, structure, and function, *Chem. Res. Toxicol. 4*, 131−140.
7. Hayes, J. D., Flanagan, J. U., and Jowsey, I. R. (2005) Glutathione transferases, *Annu. Rev. Pharmacol. Toxicol. 45*, 51−88.
8. Soberman, R. J., and Austen, K. F. (1989) The cell biology and biochemistry of leukotriene C_4 biosynthesis, *Adv. Prostaglandin Thromboxane Leukotrienes Res. 19*, 21−25.
9. Waxman, D. J. (1990) Glutathione S-transferases: role in alkylating agent resistance and possible target for modulation chemotherapy − a review, *Cancer Res. 50*, 6449−6454.
10. Ji, X., Zhang, P., Armstrong, R. N., and Gilliland, G. L. (1992) The three-dimensional structure of a glutathione S-transferase from the mu gene class. Structural analysis of the binary complex of isoenzyme 3−3 and glutathione at 2.2-Å resolution, *Biochemistry 31*, 10169−10184.
11. Wilce, M. C., and Parker, M. W. (1994) Structure and function of glutathione S-transferases, *Biochim. Biophys. Acta 1205*, 1−18.
12. Ji, X., von Rosenvinge, E. C., Johnson, W. W., Tomarev, S. I., Piatigorsky, J., Armstrong, R. N., and Gilliland, G. L. (1995) Three-dimensional structure, catalytic properties, and evolution

of a sigma class glutathione transferase from squid, a progenitor of the lens S-crystallins of cephalopods, *Biochemistry 34*, 5317−5328.
13. Hornby, J. A., Codreanu, S. G., Armstrong, R. N., and Dirr, H. W. (2002) Molecular recognition at the dimer interface of a class mu glutathione transferase: Role of a hydrophobic interaction motif in dimer stability and protein function, *Biochemistry 41*, 14238−14247.
14. Codreanu, S. G., Thompson, L. C., Hachey, D. L., Dirr, H. W., and Armstrong, R. N. (2005) Influence of the dimer interface on glutathione transferase structure and dynamics revealed by amide H/D exchange mass spectrometry, *Biochemistry 44*, 10605−10612.
15. Sinning, I., Kleywegt, G. J., Cowan, S. W., Reinemer, P., Dirr, H. W., Huber, R., Gilliland, G. L., Armstrong, R. N., Ji, X., Board, P. G., Olin, B., Mannervik, B., and Jones, T. A. (1993) Structure determination and refinement of human alpha class glutathione transferase A1-1 and a comparison with the mu and pi class enzymes, *J. Mol. Biol. 232*, 192−212.
16. Hayes, J. D., and Pulford, D. J. (1995) The glutathione S-transferase supergene family: regulation of GST and the contribution of the isoenzymes to cancer chemoprotection and drug resistance, *Crit. Rev. Biochem. Mol. Biol. 30*, 445−600.
17. Pettigrew, N. E., and Colman, R. F. (2001) Heterodimers of glutathione S-transferase can form between isoenzyme classes pi and mu, *Arch. Biochem. Biophys. 396*, 225−230.
18. Sambrook, J., Fritsch, E. F., and Maniatis, T. (1989) *Molecular Cloning: A Laboratory Manual*, 2nd ed., Cold Spring Harbor Laboratory Press, Cold Spring Harbor, NY.
19. Hearne, J. L., and Colman, R. F. (2005) Delineation of xenobiotic substrate sites in rat glutathione S-transferase M1-1, *Protein Sci. 14*, 2526−2536.
20. Vargo, M. A., Nguyen, L., and Colman, R. F. (2004) Subunit interface residues of glutathione S-transferase A1-1 that are important in the monomer−dimer equilibrium, *Biochemistry 43*, 3327−3335.
21. Schneider, J. P., Lear, J. D., and DeGrado, W. F. (1997) A designed buried salt bridge in a heterodimeric coiled coil, *J. Am. Chem. Soc. 119*, 5742−5743.
22. Kretsinger, J. K., and Schneider, J. P. (2003) Design and application of basic amino acids displaying enhanced hydrophobicity, *J. Am. Chem. Soc. 125*, 7907−7913.
23. Vargo, M. A. and Colman, R. F. (2004) Heterodimers of wild-type and subunit interface mutant enzymes of glutathione S-transferase A1−1: interactive or independent active sites? *Protein Sci. 13*, 1586−1593.
24. Habig, W. H., Pabst, M. J., and Jakoby, W. B. (1974) Glutathione S-transferases. The first enzymatic step in mercapturic acid formation, *J. Biol. Chem. 249*, 7130−7139.
25. Cacace, M. G., Landau, E. M., and Ramsden, J. J. (1997) The Hofmeister series: salt and solvent effects on interfacial phenomena, *Q. Rev. Biophys. 30*, 241−277.
26. von Hippel, P. H., and Wong, K. Y. (1965) On the conformational stability of globular proteins. The effects of various electrolytes and nonelectrolytes on the thermal ribonuclease transition, *J. Biol. Chem. 240*, 3909−3923.
27. Chou, P. Y., and Fasman, G. D. (1978) Empirical prediction of protein conformation, *Annu. Rev. Biochem. 47*, 251−76.
28. Lou, J.-K., Hornby, J. A., Wallace, L. A., Chen, J., Armstrong, R. N., and Dirr, H. W. (2002) Impact of domain interchange on conformational stability and equilibrium folding of chimeric class μ glutathione transferases, *Protein Sci. 11*, 2208−2217.
29. de Groot, M. J., Vermeulen, N. P., Mullenders, D. L., and Donne-Op den Kelder, G. M. A homology model for rat mu class glutathione S-transferase 4-4, *Chem. Res. Toxicol. 1*, 28−40.
30. Freifelder, D. (1982) *Physical Biochemistry: Applications to Biochemistry and Molecular Biology*, 2nd ed., p 13, W. H. Freeman and Company, San Francisco.
31. Cantor, C. R., and Schimmel, P. R. (1980) *Biophysical Chemistry. Part I: The Conformation of Biological Macromolecules*, W. H. Freeman and Company, San Francisco.
32. Ramos, C. H., and Baldwin, R. L. (2002) Sulfate anion stabilization of native ribonuclease A both by anion binding and by the Hofmeister effect, *Protein Sci. 11*, 1771−1778.
33. Perez-Jimenez, R., Godoy-Ruiz, R., Ibarra-Molero, B., and Sanchez-Ruiz, J. M. (2004) The efficiency of different salts to screen charge interactions in proteins: a Hofmeister effect? *Biophys. J. 86*, 2414−2429.
34. Mills, D. A., Geren, L., Hiser, C., Schmidt, B., Durham, B., Millett, F., and Ferguson-Miller, S. (2005) An arginine to lysine mutation in the vicinity of the heme propionates affects the redox potentials of the hemes and associated electron and proton transfer in cytochome *c* oxidase, *Biochemistry 44*, 10457−10465.
35. Adang, A. E. P., Brussee, J., van der Gen, A., and Mulder, G. J. (1990) The glutathione-binding site in glutathione S-transferases, *Biochem. J. 269*, 47−54.
36. Adang, A. E. P., Duindam, A. J. G., Brussee, J., Mulder, G. J., and van der Gen, A. (1988) Synthesis and nucleophilic reactivity of a series of glutathione analogues, modified at the gamma-glutamyl moiety, *Biochem J. 225*, 715−720.
37. Adang, A. E. P., Brussee, J., Meyer, D. J., Coles, B., Ketterer, B., van der Gen, A., and Mulder, G. J. (1988) Substrate specificity of rat liver glutathione S-transferase isoenzymes for a series of glutathione analogues, modified at the gamma-glutamyl moiety, *Biochem J. 255*, 721−724.
38. Xiao, G., Liu, S., Ji, X., Johnson, W. W., Chen, J., Parsons, J. F., Stevens, W. J., Gilliland, G. L., and Armstrong, R. N. (1996) First-sphere and second-sphere electrostatic effects in the active site of a class mu glutathione transferase, *Biochemistry 35*, 4753−4765.
39. Thompson, L. C., Walters, J., Burke, J., Parsons, J. F., Armstrong, R. N., and Dirr, H. W. (2006) Double mutation at the subunit interface of glutathione transferase rGSTM1-1 results in a stable, folded monomer, *Biochemistry 45*, 2267−2273.

BI060249E